

1 Revision 3

2
3 Thermochemistry of the alkali feldspars: Calorimetric study of the entropy
4 relations in the low albite – low microcline series

5 A. Benisek ¹⁾, E. Dachs ¹⁾, H. Kroll ²⁾

6
7 ¹⁾ Materialforschung und Physik, Universität Salzburg, Hellbrunnerstr. 34, 5020 Salzburg

8 ²⁾ Institut für Mineralogie, Westfälische Wilhelms Universität, Corrensstr. 24, 48149 Münster

9

10 **Abstract**

11 New heat capacity data obtained on twelve samples of the low albite – low microcline
12 series are presented. They were measured by relaxation and differential scanning
13 calorimetry between 5 and 773 K. Two series, differing in their starting materials,
14 were investigated, both of which were prepared via molten salt and solid-solid ion-
15 exchange techniques in previous studies. The heat capacity of both series deviates
16 positively from the ideal behaviour leading to positive excess vibrational entropies of
17 mixing, which can be described by a Margules mixing model yielding $W_{AbOr}^S = 8.60$
18 and $W_{OrAb}^S = 9.28 \text{ J mol}^{-1} \text{ K}^{-1}$. The heat capacity and the vibrational entropy obtained
19 on these Al,Si ordered samples are compared with those described in the literature
20 for disordered samples. The solvi of the Al,Si ordered and disordered alkali feldspar
21 systems were calculated from the calorimetric data and compared to experimentally
22 determined solvi. Large deviations are detected for the ordered system, whereas
23 consistent results are found for the disordered system, provided Na,K clustering is
24 taken into account.

25 Keywords: Low-temperature heat capacity; NaAlSi₃O₈; KAlSi₃O₈; enthalpy; mixing
26 model; miscibility gap.

27

28 **Introduction**

29 The heat capacity (C_P) of a solid solution has often been found to deviate from that of
30 a mechanical mixture (ideal mixing) at low temperatures (~ 100 K) giving rise to
31 excess vibrational entropies. Al,Si disordered alkali feldspars are characterised by
32 positive excess vibrational entropies of up to $2.5 \text{ J mol}^{-1} \text{ K}^{-1}$ (Haselton et al. 1983). In
33 high structural state plagioclases, positive excess vibrational entropies of up to 2.8 J
34 $\text{mol}^{-1} \text{ K}^{-1}$ were measured by Benisek et al. (2009), whereas an almost ideal
35 vibrational behaviour was found for the low structural state plagioclases at 298.15 K
36 (Benisek et al. 2013). The K – Ca feldspar binary, although derived from high
37 structural state plagioclases, is also characterised by a more or less ideal vibrational
38 entropy-composition relation (Benisek et al. 2010a). On the other hand, strongly
39 positive vibrational entropy behaviour has been found in ternary series of high
40 structural state feldspars (Benisek et al. 2010b). Although the origin of these excess
41 vibrational entropies is the heat capacity behaviour at low temperatures, it has a
42 strong influence on the stability of crystalline solutions at high temperatures, as
43 worked out by Benisek et al. (2010c) for the ternary Na–K–Ca feldspar system.

44 In an attempt to explain the source of the excess vibrational entropy, first
45 principles studies proposed a “bond stiffness versus bond length” interpretation (Van
46 de Walle and Ceder 2002, Burton and van de Walle 2006). The latter study
47 compared the MgO – CaO and NaCl – KCl solid solutions and found a similar size
48 mismatch but different excess vibrational behaviour, which was attributed to different
49 bond stiffness relations. The Na – Cl bonds were significantly softened with
50 increasing K content producing the positive excess vibrational entropy. Benisek and
51 Dachs (2011, 2012) presented a relationship that allows to assess the excess
52 vibrational entropy of a binary solid solution. It is based on the idea that the elastically

2

53 stiffer end member forces the softer one to fit to its size. Accordingly, the excess
54 vibrational entropy was related to the difference between the end member volumes
55 (ΔV) and to the difference between the end member bulk moduli (ΔK). The maximum
56 deviation from ideal behaviour ($\Delta_{\max} S^{\text{exc}}$) can be obtained from the relation:

$$57 \quad \Delta_{\max} S^{\text{exc}} = (\Delta V + m \Delta K) f, \quad (1)$$

58 where m and f are fit parameters. ΔV is defined to be positive, whereas ΔK may be
59 positive or negative depending on which end member (larger or smaller) is elastically
60 stiffer (i.e., $\Delta V = V_A - V_B$ and $\Delta K = K_A - K_B$, where end member A is larger than B).
61 The authors found that strongly negative ΔK values are connected with negative
62 excess vibrational entropies, whereas positive ΔK values correlate with positive ones.
63 Equation (1) could be successfully applied to different classes of materials, i.e.,
64 silicate solid solutions, binary alloys, and the NaCl – KCl binary (Benisek and Dachs
65 2011, 2012, 2013).

66 The alkali feldspars constitute a binary system consisting of the end members
67 NaAlSi₃O₈ (Ab) and KAlSi₃O₈ (Or). They represent a thoroughly investigated mineral
68 group, for which many structural, calorimetric and phase equilibrium data have been
69 obtained. The calorimetric data set, however, lacks information on the behaviour of
70 the vibrational entropy across the Al,Si ordered system. This information is provided
71 in this contribution to calculate the solvus and to compare it to the experimentally
72 determined solvus. Due to the sluggish Al,Si (dis)ordering kinetics, the Al,Si ordering
73 states of the samples that delineate the experimental solvi are not in equilibrium with
74 temperature. Thus, solvi determined from Al,Si disordered and ordered samples are
75 metastable with respect to their Al,Si distribution whereas calculation of the
76 equilibrium solvus would require knowledge of the temperature variation of the state
77 of the Al,Si order. An equilibrium solvus was estimated by Brown and Parsons (1984)

78 by interpolating data from Smith and Parsons (1974), Müller (1971) and Bachinski
79 and Müller (1971). In this paper, we calculate solvi for both the Al,Si disordered and
80 ordered alkali feldspar systems from calorimetric data and compare these to
81 experimentally determined ones.

82 Experimentally determined solvus data incorporate in principle three
83 quantities, i.e., the excess enthalpy, the excess configurational entropy and the
84 excess vibrational entropy. The calorimetrically determined solvus, on the other hand,
85 is usually based on the assumption of a fully disordered Na,K distribution free of
86 excess configurational entropy contributions. Comparing these solvi delivers,
87 therefore, information on the configurational entropy referring to the question whether
88 Na and K are in fact fully disordered or do they possess short-range ordering
89 (clustering). For the disordered alkali feldspar system, Hovis et al. (1991) performed
90 already such a comparison. To achieve agreement between calorimetric data and the
91 experimentally determined solvus, the authors reduced the calorimetrically measured
92 positive excess entropy of mixing by introducing effects of Na,K short-range ordering
93 as deduced from NMR measurements by Phillips et al. (1988).

94

95

96 **Experimental methods**

97 Alkali feldspars

98 The investigated alkali feldspars were prepared via molten salt and solid-solid ion-
99 exchange techniques (for details see for example Orville 1967). Seven samples (X_{Or}
100 = 0.01, 0.17, 0.33, 0.49, 0.66, 0.83, 1) had already been investigated by X-ray
101 diffraction and solution calorimetry in the study of Hovis (1988). For this series, low
102 albite from Amelia Courthouse, Virginia, was used as parent material. The Amelia
103 albite is a pegmatitic cleavelandite described in Waldbaum and Robie (1971) and

104 Sinkankas (1968). From the Amelia albite, a low microcline was prepared by ion-
105 exchange in molten KCl, for which we use the terminology “K-derivative of the Amelia
106 albite”. Mixtures of the end members were then homogenised at elevated
107 temperatures producing solid solution samples. The synthesis histories are given in
108 detail by Hovis (1986) and are briefly summarised in Table 1. Five samples ($X_{Or} = 0,$
109 $0.3, 0.55, 0.75, 1$) had been prepared by Kroll et al. (1986) using low albite (from a
110 metamorphic pegmatite from Cazadero, California) and a transformation-twinned low
111 microcline (perthitic amazonite from Prilep, Macedonia). The Prilep microcline was
112 first treated in molten KCl to produce pure low microcline. Solid solutions were then
113 obtained by homogenising mixtures of Cazadero albite and K-exchanged Prilep
114 microcline. The samples were characterised by X-ray diffraction in Kroll et al. (1986).
115 For preparation details of these samples see Table 1 and in more detail their study.

116

117 Relaxation calorimetry

118 The low temperature heat capacity was measured with a relaxation calorimeter
119 (Physical Properties Measurements System (PPMS); Quantum Design®) between 5
120 and 300 K using a measuring technique which is described, e.g., by Dachs and
121 Bertoldi (2005), Benisek et al. (2010b), Dachs et al. (2010), and Dachs and Benisek
122 (2011). The sample powder (~10 mg) was put into an Al cup (~8 mg) made from an
123 Al-foil. It was pressed to a cylindrical pellet (0.5 mm thickness, 5 mm in diameter), the
124 Al-foil surrounding the sample powder. The pellet was then attached to the sample
125 platform. From each sample up to three pellets were prepared and measured.

126

127 Differential scanning calorimetry

128 The heat capacity at higher temperatures was measured with a differential scanning
129 calorimeter from Perkin Elmer (Diamond DSC®). The method used in this study is

130 given elsewhere (e.g., Benisek et al. 2009, 2010a, Dachs and Benisek 2011, Benisek
131 et al. 2012). Most measurements were performed between 273 and 773 K (some
132 were performed up to only 373 K) on samples weighing approximately 25 mg. Each
133 sample was prepared in up to three different pans, each of which was measured
134 three times.

135

136 Evaluation of the heat capacity data

137 At room temperature, our DSC method provides C_P mean values of high accuracy
138 (deviating less than 0.6% from the “true” values, Dachs and Benisek 2011). On the
139 other hand, the PPMS data collected from powder samples systematically deviate
140 from the “true” values up to 2% (Dachs and Bertolid 2005). The relative deviation,
141 however, was nearly constant over the whole temperature range, when considering a
142 single PPMS run. This behaviour enables a correction where all PPMS heat capacity
143 values are multiplied by a constant factor, thereby yielding a smooth link to the DSC
144 data (Dachs and Benisek 2011). Such correction enables an improved accuracy of
145 the PPMS data as demonstrated on different oxide and silicate samples by Dachs
146 and Benisek (2011). It was also applied successfully in various solid solution studies
147 (Benisek et al. 2009, 2010a, 2010b, 2013), thereby reducing the scatter of the
148 entropy data. The correction procedure was applied in a statistical way forming all
149 possible combinations of the different PPMS and DSC data series, which resulted in
150 up to nine PPMS data series, from which the means and standard deviations were
151 calculated.

152

153 Calculation of the solvus

154 At a given equilibrium temperature and pressure, two alkali feldspars AF1 and AF2,
155 separated by the miscibility gap, have the same chemical potential for both

156 components, Ab and Or ($\mu_{Ab}^{AF1} = \mu_{Ab}^{AF2}$ and $\mu_{Or}^{AF1} = \mu_{Or}^{AF2}$). Using experimentally
157 determined mixing parameters and solving the two equations simultaneously, the
158 common tangent to the Gibbs free energy of mixing function is found. The
159 calculations for this paper used a Mathematica® routine, which searched the
160 compositions of the coexisting alkali feldspars numerically. In order to investigate the
161 uncertainties of the solvus, a Monte Carlo method was used. 10^4 sets of mixing
162 parameters were generated which were normally distributed about the experimentally
163 determined values according to the respective standard deviations. Using these
164 parameter sets, 10^4 solvi were calculated from which the standard deviation of the
165 solvus temperature at a given mole fraction could be obtained.

166

167 **Results and discussion**

168 Heat capacity of the alkali feldspars

169 The heat capacities of the investigated samples are available as electronic
170 supplementary materials from the homepage of this journal. The excess heat
171 capacity of mixing (ΔC_p^{exc}) for the alkali feldspars is defined as

$$172 \Delta C_p^{exc} = C_p^{alk\ feldspar} - (C_p^{Ab} X_{Ab} + C_p^{Or} X_{Or}). \quad (2)$$

173 An example is given for an intermediate composition in Figure 1. In the low
174 temperature region, ΔC_p^{exc} of all Al,Si ordered samples is positive reaching a
175 maximum of $1.2\text{ J mol}^{-1}\text{ K}^{-1}$ at $\sim 85\text{ K}$. At $\sim 300\text{ K}$, the data of the ordered $Ab_{51}Or_{49}$
176 sample suggest a negative peak ($-0.7\text{ J mol}^{-1}\text{ K}^{-1}$) which, however, may not be
177 significant ($1\text{ s.d.}^{(300K)} \approx 0.4\text{ J mol}^{-1}\text{ K}^{-1}$). The results of Haselton et al. (1983) obtained
178 on a sample with a similar composition, $Ab_{55}Or_{45}$, but with a disordered Al,Si
179 distribution, are added in Figure 1 for comparison. Both samples show similar excess
180 heat capacity behaviour. The disordered sample, however, has no negative peak at
181 $\sim 300\text{ K}$ and has its maximum positive peak at a slightly lower temperature ($\sim 70\text{ K}$).

7

182

183 Vibrational entropy of the alkali feldspars

184 The vibrational entropy at 298.15 K

$$185 \quad S^{298.15} - S^0 = \int_0^{298.15} (C_P^{\text{alk feldsp}} / T) \partial T \quad (3)$$

186 of the low albite – low microcline series is shown in Figure 2 and listed in Table 2.

187 Jointly fitting all data to an asymmetric Margules mixing model resulted in interaction

188 parameters $W_{\text{AbOr}}^S = 8.60$ and $W_{\text{OrAb}}^S = 9.28 \text{ J mol}^{-1} \text{ K}^{-1}$, showing only a small

189 asymmetric behaviour. At 400 K, the excess vibrational entropy is slightly smaller

190 than that at 298.15 K, the difference being less than one standard deviation.

191 If samples prepared from Amelia albite ($X_{\text{Or}} = 0.01, 0.17, 0.33, 0.49, 0.66,$

192 $0.83, 1$) are considered separately from those prepared from Cazadero albite and

193 Prilep microcline ($X_{\text{Or}} = 0, 0.30, 0.55, 0.75$ and 1), a slightly different behaviour

194 arises. In the Ab-rich region, the Amelia albite series shows slightly larger entropy

195 values (Fig. 2), although the deviation from the Cazadero albite – Prilep microcline

196 series lies within uncertainties. However, because the Amelia albite series has

197 enthalpy values that are significantly different from other low albite – low microcline

198 series (see below), the vibrational entropy values were fitted separately. Because of

199 the low number of data and the very small asymmetry, a symmetric Margules mixing

200 model was used. For the Amelia albite series, the separate fitting procedure resulted

201 in $W^S = 8.7 \pm 1.1 \text{ J mol}^{-1} \text{ K}^{-1}$, while the Cazadero albite – Prilep microcline series has

202 slightly higher excess entropy values yielding $W^S = 9.1 \pm 1.4 \text{ J mol}^{-1} \text{ K}^{-1}$.

203 The vibrational entropy results from this study are similar to those obtained on

204 samples with a disordered Al,Si distribution (Haselton et al. 1983), as seen in Fig. 2.

205 Compared to the samples of the Amelia albite series the disordered samples have

206 lower entropy values in the Ab-rich region, but agree well with those of the Cazadero

207 albite – Prilep microcline series. The disordered series has a maximum excess
208 vibrational entropy $\Delta_{\max}S^{\text{exc}} = 2.5 \text{ J mol}^{-1} \text{ K}^{-1}$. In the ordered series the mean value of
209 $\Delta_{\max}S^{\text{exc}}$ is slightly smaller ($2.3 \text{ J mol}^{-1} \text{ K}^{-1}$, this study). Thus, the entropic Na – K
210 mixing behaviour does not depend significantly on the state of Al,Si order which is in
211 contrast to the enthalpic mixing behaviour. In the analbite – sanidine series the
212 maximum excess enthalpy, $\Delta_{\max}H^{\text{exc}}$, amounts to 5.0 kJ mol^{-1} , whereas in the low
213 albite – low microcline series, $\Delta_{\max}H^{\text{exc}}$ is distinctly larger, 8.0 kJ mol^{-1} (Hovis 1988).
214 Additionally, the asymmetry of ΔH^{exc} increases with Al,Si ordering. The disordered
215 series is almost symmetric, whereas the ordered series has its maximum at $X_{\text{Or}} =$
216 0.37.

217 Studies on liquid binary alloys (e.g., Kubaschewski and Alcock 1979,
218 Witusiewicz and Sommer 2000), on alkali halide, metallic and some oxide systems
219 (Urusov et al. 2007, 2008) found a correlation between excess enthalpy and excess
220 entropy of mixing. The data of the ordered and disordered Ab – Or series do not
221 support this correlation. The excess vibrational entropy of mixing is, however, in
222 accordance with a relationship recently published by Benisek and Dachs (2011,
223 2012), which estimates the maximum value of the excess vibrational entropy based
224 on the differences between end member volumes and bulk moduli, as noted above.

225 The difference of the bulk modulus between low albite and low microcline (ΔK
226 = 5.3 GPa , Downs et al. 1994, Allan and Angel 1997) is smaller than between
227 analbite and sanidine ($\Delta K = 7.7 \text{ GPa}$, Curetti et al. 2011, Angel 1994). On the other
228 hand, low albite and low microcline have a larger difference in their molar volumes
229 ($\Delta V = 0.884 \text{ J bar}^{-1}$, Kroll and Ribbe 1983) compared to analbite and sanidine ($\Delta V =$
230 0.858 J bar^{-1} , Kroll and Ribbe 1983). Using equation (1) with $m = 0.0109$ and $f =$
231 2.505 (Benisek and Dachs 2012), the estimated maximum excess vibrational

232 entropies are the same in both series, i.e., $\Delta_{\max}S^{\text{exc}} = 2.4 \text{ J mol}^{-1} \text{ K}^{-1}$, which is in good
233 agreement with the experimental results. The positive excess vibrational entropy may
234 be explained by large Na – O bond lengths in samples with intermediate
235 compositions owing to the presence of the elastically stiffer and larger K – O
236 polyhedra. This effect decreases strongly the stiffness of the Na – O bonds and, in
237 consequence, the frequency of the Na – O vibrations, which are then excited at lower
238 temperatures giving rise to positive excess heat capacities of mixing. The large
239 increase of the Na – O bond lengths with the Na – K substitution is consistent with
240 results from ^{23}Na NMR investigation of samples of the Al,Si ordered alkali feldspar
241 series (Phillips et al. 1988).

242

243 Excess enthalpy of mixing

244 To calculate the solvus of the Ab – Or system, the excess enthalpy and volume of
245 mixing have to be known in addition to the excess entropy of mixing. In Figure 3, the
246 enthalpy of solution in hydrofluoric acid for three different alkali feldspar series is
247 plotted as a function of composition. Two different Al,Si ordered series can be
248 compared, i.e., the one of Hovis (1988) (see Table 1 for preparation details) and the
249 one of Waldbaum and Robie (1971). The latter series was also prepared by the
250 molten salt and solid-solid ion-exchange techniques. However, Waldbaum and Robie
251 (1971) used Amelia microcline as parent material, a sample twinned due to the
252 diffusive Al,Si ordering transformation, whereas Hovis (1988) investigated samples
253 prepared from Amelia albite – a sample free of transformation twinning. Their
254 investigations yielded significantly different enthalpy values (Fig. 3). The results of
255 Hovis (1988) show larger enthalpy values with a maximum deviation from ideal
256 behaviour of $\Delta_{\max}H^{\text{exc}} = 8.0 \text{ kJ mol}^{-1}$ at $X_{\text{Or}} = 0.37$, whereas Waldbaum and Robie
257 (1971) measured a maximum deviation of $\Delta_{\max}H^{\text{exc}} = 7.5 \text{ kJ mol}^{-1}$ at $X_{\text{Or}} = 0.43$. The

10

258 excess behaviour measured by Waldbaum and Robie (1971) is thus smaller and
259 more symmetric compared to Hovis (1988). Waldbaum and Robie (1971) also
260 investigated two samples ($X_{Or} = 0$ and 1), which were prepared from Amelia albite.
261 For these samples, excellent agreement (Fig. 3) can be found with the results of
262 Hovis (1988), also based on Amelia albite. The different results for the Al,Si ordered
263 series visible in Figure 3 are, thus, due to the use of different parent materials for
264 preparing the solid solution series. In Figure 3, the enthalpies of solution for the
265 analbite – sanidine series are also shown, which are characterised by larger values,
266 but a smaller maximum deviation from ideal behaviour ($\Delta_{max}H^{exc} = 5.0 \text{ kJ mol}^{-1}$).

267 Cation mixing due to formation of a solid solution produces local structural
268 distortions and in consequence strain energies (e.g., Christian 1975, Greenwood
269 1979), which is true for cation disordering as well. These strain energies should be
270 reflected in changes of the enthalpy. To discuss the enthalpic data of the alkali
271 feldspars (Fig. 3), let us first consider the Na end member as an example: Analbite
272 has the largest negative enthalpy of solution value followed by the Amelia albite and
273 then by the Na-derivative of the Amelia microcline. Considering their enthalpies of
274 formation, the opposite is true, i.e., analbite has the less negative value followed by
275 the other two. The relationship between enthalpy of solution and formation is
276 sketched in Figure 4 for these Na-feldspars. The sum of all bond energies is thus
277 smallest in analbite. This is certainly due to the bond energies being lowered by the
278 strain energies present in the disordered structure. The situation for the Amelia albite
279 and the Na-derivative of the Amelia microcline is somewhat surprising. Although the
280 Na-derivative of the Amelia microcline is characterised by transformation twinning
281 and hence by strain energies due to twin walls, the enthalpy of formation has the
282 largest negative value, i.e., the sum of all bond energies is largest. The Amelia albite
283 is obviously characterised by larger structural strain. This behaviour may be

284 explained by a higher defect concentration. Amelia albite is a cleavelandite – a
285 feldspar variety with curved or warped plates.

286 The same considerations are true for the K-feldspars (Fig. 3). The structural
287 heterogeneities caused by Na – K mixing also produce local elastic strain and
288 consequently positive deviations from ideal enthalpic behaviour. The excess enthalpy
289 of mixing is largest in the ordered series with Amelia albite as parent material, slightly
290 lower in the other ordered series prepared from Amelia microcline, and smallest in
291 the disordered series. The smaller excess enthalpy in the disordered series may be
292 explained by the fact that the structure is “held open” due to the Al,Si disorder so that
293 the local elastic strain due to Na – K mixing is less effective.

294

295 The low albite – low microcline solvus

296 The solvus for the Ab – Or system with an ordered Al,Si distribution was calculated
297 using two different thermodynamic data sets, one derived from the Amelia albite
298 series (ordered feldspar data set 1, Table 3), the other derived from the Amelia
299 microcline series for the enthalpy and the Cazadero albite – Prilep microcline series
300 for the entropy and volume (ordered feldspar data set 2, Table 3). The configurational
301 entropy was calculated using the one-site mixing model, which assumes Na,K to be
302 fully disordered.

303 When calculating the ordered feldspar solvus using data set 1, a critical
304 temperatures of $1510 \pm 110^\circ\text{C}$ is obtained, while the data set 2 results in $T_{\text{crit}} = 990 \pm$
305 100°C (Fig. 5). The difference arises mainly from the different enthalpic data
306 (previous chapter). Experimentally determined solvi (Bachinski and Müller 1971,
307 Delbove 1975) yielded $T_{\text{crit}} \sim 886^\circ\text{C}$. The solvus calculated from data set 1 ($T_{\text{crit}} =$
308 1510°C) is in clear conflict with these data and with the temperature of 1000°C ,
309 which proved to be sufficiently high in order to prepare homogeneous intermediate

12

310 compositions ($0.2 \leq X_{Or} \leq 0.6$) (Kroll et al. 1986). The reason for the discrepancy is
311 not clear. A possible explanation could be that the samples used for data set 1, which
312 were prepared from Amelia albite possess a higher density of imperfections than do
313 the samples for data set 2. The additional configurational entropy is not considered in
314 the solvus calculation, but would lower the solvus when incorporated into the
315 calculation. In contrast, the solvus of data set 2 is in agreement with both the
316 homogenisation temperature of 1000°C and the experimentally determined solvus,
317 provided the uncertainties are taken into account (Fig. 5).

318 If our solvus calculations would incorporate a configurational entropy model
319 that includes Na,K clustering, which was found in ordered alkali feldspars
320 homogenised at 930°C (Phillips et al. 1988), the solvus calculated from data set 2
321 would become clearly larger than the solvus of Bachinski and Müller (1971). On the
322 other hand, results from older solvus studies (e.g., Spencer 1937, Goldsmith and
323 Laves 1961) indicate critical temperatures higher than 1000°C, which may then
324 become comparable with the calculated solvus using data set 2 when incorporating
325 Na,K clustering. The effect of clustering on the solvus is discussed below.

326

327 The analbite – sanidine solvus

328 To calculate the solvus of the disordered system, the data of Hovis (1988) and
329 Haselton et al. (1983) were used. They were measured on alkali feldspar series,
330 which were prepared from Al,Si disordered Amelia albite (Table 3). Defects, which
331 may exist in the Al,Si ordered samples, are expected to be annihilated during the
332 Al,Si disordering procedure (e.g., 1052°C, 710 hours, for producing analbite from low
333 albite, Hovis 1977). The resulting solvus has a critical temperature of $490 \pm 25^\circ\text{C}$,
334 which is lower than indicated by the experimentally determined solvus (e.g.,
335 Goldsmith and Newton 1974, Smith and Parsons 1974, Parsons 1978, Lagache and

336 Weisbrod 1977). The difference in the critical temperatures is $\sim 160^{\circ}\text{C}$ as seen from
337 Figure 6. If, however, the configurational entropy resulting from the Na,K distribution
338 is decreased in the Ab-rich compositional region by a maximum of $1.0 \text{ J mol}^{-1} \text{ K}^{-1}$, as
339 shown in Fig. 7, good agreement between calculation and experiment is obtained
340 (Fig. 6). Such a decrease can be generated assuming Na,K clustering/ordering to be
341 present. Phillips et al. (1988) investigated Al,Si ordered alkali feldspars homogenised
342 at 930°C . Their ^{23}Na NMR spectra especially of Ab-rich samples indicate that the
343 Na,K environment of a Na atom is skewed toward a relative enrichment of Na atoms
344 (Phillips et al., 1988), which we will term “short-range clustering”. Such clustering
345 above the solvus was also found in many metallic systems (e.g., Rudman and
346 Averbach 1954, Sakakibara et al. 1994). A similar behaviour is also to be expected in
347 disordered alkali feldspar samples close to the solvus. The solvus calculated from the
348 calorimetric data without considering short-range clustering (*solid line* in Fig. 6) thus
349 represents a hypothetical solvus with the two coexisting alkali feldspars being fully
350 disordered with respect to Na,K. Accordingly, a homogenous $\text{Ab}_{60}\text{Or}_{40}$ crystal for
351 example would be stable at 500°C only if its Na,K distribution were fully disordered.
352 However, Na,K short-range clustering present in such a crystal decreases the
353 configurational entropy which destabilises the solid solution raising the solvus to the
354 experimentally observed temperatures. Investigation on the NaCl – KCl crystalline
355 solution (Benisek and Dachs, 2013) shows that a similar amount of short-range
356 clustering ($\sim 0.5 \text{ J mol}^{-1} \text{ K}^{-1}$ in the Na-rich compositional region) has to be assumed to
357 obtain agreement between the calorimetrically determined solvus and the one
358 bracketed by Na – K exchange experiments.

359 The excess enthalpy and the excess vibrational entropy of mixing were
360 measured on Al,Si disordered samples, whose Na,K short-range clustering is to be
361 expected to be less pronounced (homogenised at 930°C) than in samples used to

362 experimentally determine the solvus (at $T < 650^{\circ}\text{C}$). The excess vibrational entropy
363 decreases slightly with an increase of the Na,K clustering, as found from DFT lattice
364 dynamics calculations (Benisek and Dachs, in preparation). The excess enthalpy,
365 too, is to be expected to be smaller in samples with a more pronounced clustering. A
366 full description of the solvus samples would need, therefore, not only a reduction of
367 the configurational entropy due to Na,K clustering, as done here, but also the effect
368 of this reduction on the excess enthalpy and vibrational entropy.

369 The solvus samples in Fig. 5 and 6 represent alkali feldspars whose Na,K
370 distribution is equilibrated, which is, however, not the case concerning their Al,Si
371 distribution. The samples that have been used to determine the disordered alkali
372 feldspar solvus have a larger degree of Al,Si disorder than required by the solvus
373 temperatures. The Al,Si distribution of the samples of the ordered alkali feldspar
374 solvus, on the other hand, is relatively too ordered, especially at the critical
375 temperature. As mentioned above, an equilibrium solvus was estimated by Brown
376 and Parsons (1984) by interpolating data from experimental solvi with different Al,Si
377 order (Smith and Parsons 1974, Müller 1971, Bachinski and Müller 1971).

378

379

380 **Implications**

381 The investigation of the entropic behaviour of the Al,Si ordered and disordered alkali
382 feldspars confirms a model describing the nature of the excess entropy of mixing that
383 can be applied not only in geosciences, but also in other fields like metallurgy.

384 The mixing properties of binary systems are often extracted from solvus data,
385 which were experimentally determined (e.g., Green 1970, Powell 1974, Hovis et al.
386 1991, Holland and Powell 2003). Such mixing models, however, are only valid with
387 respect to the solvus samples from which they were derived. In case of Al,Si

388 disordered alkali feldspars, the mixing parameters so derived are not suitable to
389 model the high temperature activity-composition behaviour above the solvus. The
390 equilibrium amount of Na,K short-range clustering present in samples held at
391 temperatures close to the solvus is expected to be larger than in samples held at
392 higher temperatures. The effect of this short-range clustering on the configurational
393 entropy is, therefore, smaller in equilibrated high-temperature samples than in the
394 metastable solvus samples. Many petrologic problems involve disordered alkali
395 feldspars, for which the activity composition relations need to be known at high
396 temperatures (~900°C, e.g., thermometry including ternary feldspars, melting of alkali
397 feldspar). For such alkali feldspars, we present mixing parameters in Table 3. They
398 agree within uncertainties with those incorporated into the ternary feldspar mixing
399 model of Benisek et al. (2010c) and their Excel spreadsheet for calculating two-
400 feldspar temperatures and are valid at high temperatures. For a comprehensive
401 thermodynamic description of alkali feldspars at lower temperatures, the effects of
402 Na,K short-range clustering and Al,Si ordering need to be considered. Whereas Al,Si
403 ordering could be modelled by applying e.g., the symmetric formalism of Holland and
404 Powell (1996), future studies on Na,K short-range clustering in alkali feldspars could
405 be done using drop calorimetry in order to quantify the energetics of this effect. In the
406 case of the Cu – Zn system, where ordering processes occur at lower temperatures
407 than in the alkali feldspars, the energetic effects were successfully studied by DSC-
408 methods (Benisek et al, submitted).

409

410

411 **Acknowledgement**

412 This work was supported by grants from the Austrian Science Fund (FWF), project
413 numbers P23056-N21 and P21370-N21, which is gratefully acknowledged. We thank

414 G. Hovis (Lafayette College, Easton, USA) for providing samples and for valuable
415 contributions. We also acknowledge the careful reviews of I. Parsons (University of
416 Edinburgh, UK) and an anonymous reviewer.

417

418

419 **References**

- 420 Allan, D.R. and Angel, R.J. (1997) A high-pressure structural study of microcline
421 (KAISi₃O₈) to 7 GPa. *European Journal of Mineralogy*, 9, 263-275.
- 422 Angel, R.J. (1994) Feldspars at high pressures. In Parsons I (ed), *Feldspars and their*
423 *reactions*. Kluwer Academic Publishers, Dordrecht, Boston, London, 271-312.
- 424 Bachinski, S.W. and Müller, G. (1971) Experimental determinations of the microcline
425 – low albite solvus. *Journal of Petrology*, 12, 329-356.
- 426 Benisek, A., Kroll, H., Cemič, L., Kohl, V., Breit, U., Heying, B. (2003) Enthalpies in
427 (Na,Ca)- and (K,Ca)-feldspar binaries: a high temperature solution calorimetric
428 study. *Contribution to Mineralogy and Petrology*, 145, 119-129.
- 429 Benisek, A., Dachs, E., Kroll, H. (2009) Excess heat capacity and entropy of mixing in
430 the plagioclase solid solution. *American Mineralogist*, 94, 1153-1161.
- 431 Benisek, A., Dachs, E., Kroll, H. (2010a) Excess heat capacity and entropy of mixing
432 in the high-structural state (K,Ca)-feldspar binary. *Physics and Chemistry of*
433 *Minerals*, 37, 209-218.
- 434 Benisek, A., Dachs, E., Kroll, H. (2010b) Excess heat capacity and entropy of mixing
435 in ternary series of high structural state feldspars. *European Journal of*
436 *Mineralogy*, 22, 403-410.
- 437 Benisek, A., Dachs, E., Kroll, H. (2010c) A ternary feldspar-mixing model based on
438 calorimetric data: development and application. *Contribution to Mineralogy and*
439 *Petrology*, 160, 327-337.

- 440 Benisek, A. and Dachs, E. (2011) On the nature of the excess heat capacity of
441 mixing. *Physics and Chemistry of Minerals*, 38, 185-191.
- 442 Benisek, A. and Dachs, E. (2012) A relationship to estimate the excess entropy of
443 mixing: application in silicate solid solutions and binary alloys. *Journal of*
444 *Alloys and Compounds*, 527, 127-131.
- 445 Benisek, A., Kroll, H., Dachs, E. (2012) The heat capacity of fayalite at high
446 temperatures. *American Mineralogist*, 97, 657-660.
- 447 Benisek, A., Dachs, E., Carpenter, M.A. (2013) Heat capacity and entropy of low
448 structural state plagioclases. *Physics and Chemistry of Minerals*, 40, 167-173.
- 449 Benisek, A. and Dachs E (2013) Calorimetric study of the entropy relation in the NaCl
450 – KCl system. *The Journal of Chemical Thermodynamics*, 62, 231-235.
- 451 Boffa Ballaran, T. and Carpenter, M.A. (2003) Line broadening and enthalpy: some
452 empirical calibrations of solid solution behaviour from IR spectra. *Phase*
453 *Transitions*, 76, 137-154.
- 454 Brown, W.L. and Parsons, I. (1984) Exsolution and coarsening mechanisms and
455 kinetics in an ordered cryptoperthite series. *Contributions to Mineralogy and*
456 *Petrology*, 86, 3-18.
- 457 Burton, B.P. and van de Walle, A. (2006) First-principles phase diagram calculations
458 for the system NaCl – KCl: The role of excess vibrational entropy. *Chemical*
459 *Geology*, 225, 222-229.
- 460 Carpenter, M.A., McConnell, J.D.C., Navrotsky, A. (1985) Enthalpies of ordering in
461 the plagioclase feldspar solid solution. *Geochimica et Cosmochimica Acta*, 49,
462 947-966.
- 463 Christian, J.W. (1975) *The theory of transformation in metals and alloys: An*
464 *advanced textbook in physical metallurgy*, 2nd ed., Pergamon Press, Oxford,
465 UK.

- 466 Curetti, N., Sochalski-Kolbus, L.M., Angel, R.J., Benna, P., Nestola, F., Bruno, E.
467 (2011) High-pressure structural evolution and equation of state of analbite.
468 American Mineralogist, 96, 383-392.
- 469 Dachs, E. and Bertoldi, C. (2005) Precision and accuracy of the heat-pulse
470 calorimetric technique: low-temperature heat capacities of milligram-sized
471 synthetic mineral samples. European Journal of Mineralogy, 17, 251-259.
- 472 Dachs, E., Harlov, D., Benisek, A. (2010) Excess heat capacity and entropy of mixing
473 along the chlorapatite-fluorapatite binary join. Physics and Chemistry of
474 Minerals, 37, 665-676.
- 475 Dachs, E. and Benisek A (2011) A sample-saving method for heat capacity
476 measurements on powders using relaxation calorimetry. Cryogenics, 51, 460-
477 464.
- 478 Delbove, F. (1975) Excess Gibbs Energy of microcline-low albite alkali feldspars at
479 800°C and 1 bar, based on fused alkali bromide ion-exchange experiments.
480 American Mineralogist, 60, 972-984.
- 481 Downs, R.T., Hazen, R.M., Finger, L.W. (1994) The high-pressure crystal chemistry
482 of low albite and the origin of the pressure dependency of Al – Si ordering.
483 American Mineralogist, 79, 1042-1052.
- 484 Goldsmith, J.R. and Laves, F. (1961) The sodium content of microcline and the
485 microcline – albite series. Crusillos y Conferencias, Inst. Lucas Mallada,
486 C.S.I.C, 8, 81-96.
- 487 Goldsmith, J.R. and Newton, R.C. (1974) An experimental determination of the alkali
488 feldspar solvus. In MacKenzie WS, Zussman J (Eds) The feldspars,
489 Manchester University Press, Manchester, UK, p. 337-359.
- 490 Green, E.J. (1970) Predictive thermodynamic models for mineral systems. I. Quasi-
491 chemical analysis of the halite-sylvite subsolidus. American Mineralogist, 55,

- 492 1692-1713.
- 493 Greenwood, H.J. (1979) Some linear and non-linear problems in petrology.
494 *Geochimica et Cosmochimica Acta*, 43, 1873-1885.
- 495 Haselton, H.T., Jr., Hovis, G.L., Hemingway, B.S., Robie, R.A. (1983) Calorimetric
496 investigation of the excess entropy of mixing in analbite-sanidine solid
497 solutions: lack of evidence for Na,K short-range order and implications for two-
498 feldspar thermometry. *American Mineralogist*, 68, 398-413.
- 499 Holland, T. and Powell, R. (1996) Thermodynamics of order-disorder in minerals: II.
500 Symmetric formalism applied to solid solutions. *American Mineralogist*, 81,
501 1425-1437.
- 502 Holland, T. and Powell, R. (2003) Activity-composition relations for phases in
503 petrological calculations: an asymmetric multicomponent formulation.
504 *Contribution to Mineralogy and Petrology*, 145, 492-501.
- 505 Hovis, G.L. (1977) Unit-cell dimensions and molar volumes for a sanidine-analbite
506 ion-exchange series. *American Mineralogist*, 62, 672-679,
- 507 Hovis, G.L. (1986) Behavior of alkali feldspar: Crystallographic properties and
508 characterization of composition and Al-Si distribution. *American Mineralogist*,
509 71, 869-890.
- 510 Hovis, G.L. (1988) Enthalpies and volumes related to K-Na mixing and Al-Si
511 order/disorder in alkali feldspars. *Journal of Petrology*, 29, 731-763.
- 512 Hovis, G.L., Delbove, F., Roll Bose, M. (1991) Gibbs energies and entropies of K-Na
513 mixing for alkali feldspars from phase equilibrium data: Implications for
514 feldspar solvi and short-range order. *American Mineralogist*, 76, 913-927.
- 515 Hovis, G.L. and Navrotsky A (1995) Enthalpies of mixing for disordered alkali
516 feldspars at high temperature: A test of regular solution thermodynamic
517 models and a comparison of hydrofluoric acid and lead borate solution

- 518 calorimetric techniques. American Mineralogist, 80, 280-284.
- 519 Kroll, H. and Ribbe, P.H. (1983) Lattice parameters, composition and Al,Si order in
520 alkali feldspars. In: Ribbe PH, (ed) Feldspar mineralogy, Reviews in
521 mineralogy, Mineralogical Society of America, pp. 57-98.
- 522 Kroll, H., Schiemann, I., von Cölln, G. (1986) Feldspar solid solutions. American
523 Mineralogist, 71, 1-16.
- 524 Kubaschewski, O. and Alcock, C.B. (1979) Metallurgical thermochemistry, Pergamon
525 Press, Oxford.
- 526 Lagache, M. and Weisbrod, A. (1977) The system: two alkali feldspars-KCl-NaCl-H₂O
527 at moderate to high temperatures and low pressures. Contribution to
528 Mineralogy and Petrology, 62, 77-101.
- 529 Müller, G. (1971) Der Einfluss der Al,Si-Verteilung auf die Mischungslücke der Alkali-
530 Feldspäte. Contribution to Mineralogy and Petrology, 34, 73-79.
- 531 Newton, R.C., Charlu, T.V., Kleppa, O.J. (1980) Thermochemistry of high structural
532 state plagioclases. Geochimica et Cosmochimica Acta, 44, 933-941.
- 533 Orville, P.M. (1967) Unit-cell parameters of the microcline-low albite and sanidine-
534 high albite solid solution series. American Mineralogist, 52, 55-86. Correction,
535 346-347.
- 536 Parsons, I. (1978) Alkali-feldspars: which solvus? Physics and Chemistry of Minerals,
537 2, 199-213.
- 538 Phillips, B.L., Kirkpatrick, R.J., Hovis, G.L. (1988) ²⁷Al, ²⁹Si, and ²³Na MAS NMR
539 study of an Al,Si ordered alkali feldspar solid solution series. Physics and
540 Chemistry of Minerals, 16, 262-275.
- 541 Powell, R. (1974) A comparison of some mixing models for crystalline silicate solid
542 solutions. Contribution to Mineralogy and Petrology, 46, 265-274.
- 543 Rudman, P.S. and Averbach B.L. (1954) X-ray measurements of local atomic

- 544 arrangements in aluminium-zinc and in aluminium-silver solid solutions. *Acta*
545 *metallurgica*, 2, 576-582.
- 546 Sakakibara A., Kanadani T., Nakagawa K., Yokota Y. (1994) Clusters in low-
547 concentrated Al-Mg alloy. *Memoirs Faculty Engineering, Okayama University*,
548 28, 9-12
- 549 Sinkankas, J. (1968) Classic mineral occurrences: I. Geology and mineralogy of the
550 Rutherford pegmatites, Amelia, Virginia. *American Mineralogist*, 53, 373-405.
- 551 Smith, P. and Parsons, I. (1974) The alkali-feldspar solvus at 1 kilobar water-vapour
552 pressure. *Mineralogical Magazine*, 39, 747-767.
- 553 Spencer, .E (1937) The potash – soda – feldspars. I. Thermal stability. *Mineralogical*
554 *Magazine*, 24, 453-494.
- 555 Urusov, V.S., Petrova, T.G., Leonenko, E.V. Eremin, N.N. (2007) A computer
556 simulation of halite-sylvite (NaCl-KCl) solid solution local structure, properties,
557 and stability. *Moscow University Geology Bulletin*, 62, 117-122.
- 558 Urusov, V.S., Petrova, T.G., Eremin, N.N. (2008) Computer modeling of the local
559 structure, mixing properties, and stability of solid solutions of alkaline-earth
560 metal oxides. *Crystallography Reports*, 53, 1030-1038.
- 561 Van de Walle, A. and Ceder, G. (2002) The effect of lattice vibrations on
562 substitutional alloy thermodynamics. *Review of Modern Physics*, 74, 11-45.
- 563 Waldbaum, D.R. and Robie, R.A. (1971) Calorimetric investigation of Na – K mixing
564 and polymorphism in the alkali feldspars. *Zeitschrift für Kristallographie*, 134,
565 381-420.
- 566 Witusiewicz, V.T., Sommer, F. (2000) Estimation of the excess entropy of mixing and
567 the excess heat capacity of liquid alloys, *Journal of Alloys and Compounds*,
568 312, 228-237.
- 569

570

571 **Figure Captions**

572 Fig. 1: Excess heat capacity of mixing (ΔC_p^{exc}) of samples with intermediate
573 compositions ($\text{Ab}_{\sim 50}\text{Or}_{\sim 50}$). *Closed symbols*: ordered Al,Si distribution (this work),
574 *open symbols*: disordered Al,Si distribution (Haselton et al. 1983). Error bars
575 represent 1 s.d.

576

577 Fig. 2: Vibrational entropy at $T = 298.15 \text{ K}$ ($S^{298.15} - S^0$) as a function of composition.
578 *Closed circles*: alkali feldspars prepared from Amelia albite, *closed squares*: alkali
579 feldspars prepared from Cazadero albite + Prilep microcline. The data were jointly
580 fitted to a Margules mixing model yielding $W_{\text{AbOr}}^S = 8.60$ and $W_{\text{OrAb}}^S = 9.28 \text{ J mol}^{-1} \text{ K}^{-1}$.
581 ¹. Data of the analbite – sanidine series from Haselton et al. (1983) (*open triangles*)
582 are added for comparison. Error bars represent 1 e.s.d.

583

584 Fig. 3: Enthalpies of solution in hydrofluoric acid for the Ab – Or series. *Solid circles*:
585 data from Waldbaum and Robie (1971) obtained on samples prepared from Amelia
586 microcline and thus characterised by cross-hatched microcline twinning
587 (transformation twinning). *Open triangles*: data from Hovis (1988) for samples
588 prepared from Amelia albite. *Open circles*: data from Waldbaum and Robie (1971) for
589 pure and K-exchanged Amelia albite. *Open diamonds*: data from Hovis (1988) for the
590 analbite – sanidine series.

591

592 Fig. 4: A sketch of the relationship between enthalpies of solution and formation,
593 respectively, demonstrated for different Na-feldspars (not to scale). The numbers
594 represent the enthalpy changes (kJ mol^{-1}), when Na-feldspar is dissolved in
595 hydrofluoric acid at 50°C (Hovis 1988, Waldbaum and Robie 1971) and lead borate

23

596 solvent at 700°C, respectively (Newton et al. 1980, Carpenter et al. 1985, Hovis and
597 Navrotsky 1995, Benisek et al. 2003).

598

599 Fig. 5: Calculated solvi at 1 bar for the Al,Si ordered alkali feldspar system. The solvi
600 are compared with the phase equilibrium experiments of Bachinski and Müller (1971)
601 (*open diamonds*) and Delbove (1975) (*closed diamonds*). The calculations used two
602 different thermodynamic data sets. The data set of ordered feldspar 1 (Table 3) is
603 given by the upper *solid curve*, that of ordered feldspar 2 (Table 3) by the lower solid
604 curve. A Monte Carlo method was used to investigate the uncertainty of the
605 calculated solvi which is represented by the dashed lines (1 s.e.d.). Liquidus and
606 solidus curves are not shown.

607

608 Fig. 6: Solvi at 1 kbar for the Al,Si disordered alkali feldspar system. *Solid curve*:
609 Calculated solvus with uncertainties (dashed lines) based on calorimetric data from
610 Hovis (1988) and Haselton et al. (1983); the interaction parameters used are listed in
611 Table 3. *Dash-dotted curve*: same interaction parameters, however, accounting for
612 Na,K short-range clustering as shown in Fig. 7. Phase equilibrium experiments are
613 taken from Smith and Parsons (1974) and Parsons (1978) (*arrows*), and from
614 Lagache and Weisbrod (1977) (*bars with dots*). They are consistent with high
615 pressure solvus data (9 -15 kbar) from Goldsmith and Newton (1974), when the
616 volumetric mixing parameters of e.g., Kroll et al. (1986), Hovis (1988), or Hovis et al.
617 (1991) are used.

618

619 Fig. 7: Configurational entropy (S^{cfg}) in the alkali feldspar series. *Solid line*: One site
620 mixing model (= disordered Na,K distribution). *Broken line*: Reduction due to Na,K

- 621 short-range clustering in the Ab-rich region, described with a Margules mixing model
- 622 using $W_{OrAb} = -7$, $W_{AbOr} = 0 \text{ J mol}^{-1} \text{ K}^{-1}$.

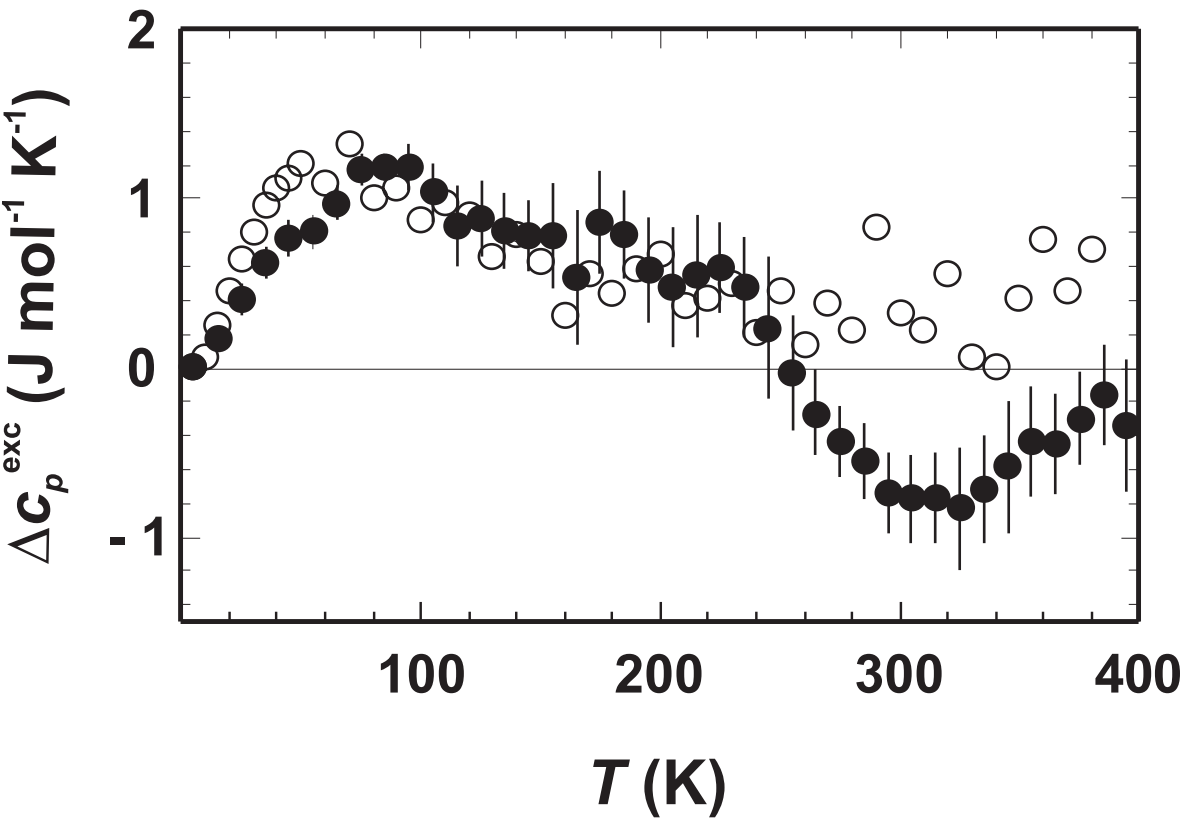


Fig. 1

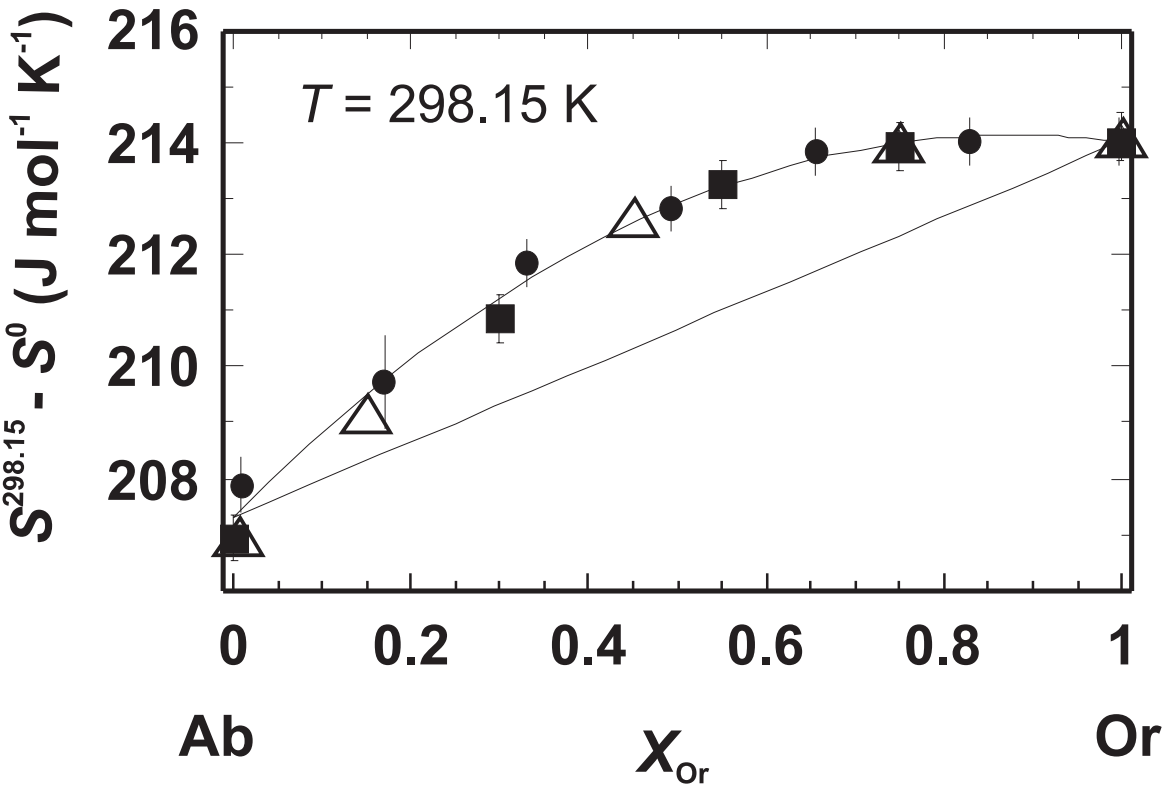


Fig. 2

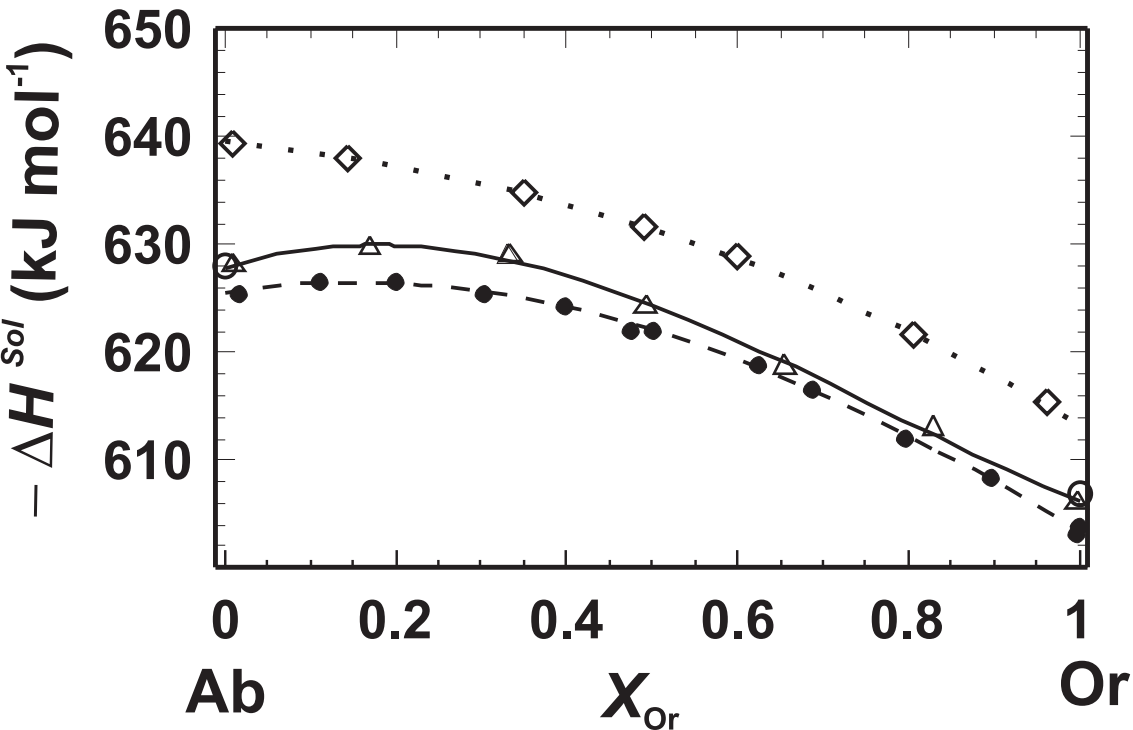


Fig. 3

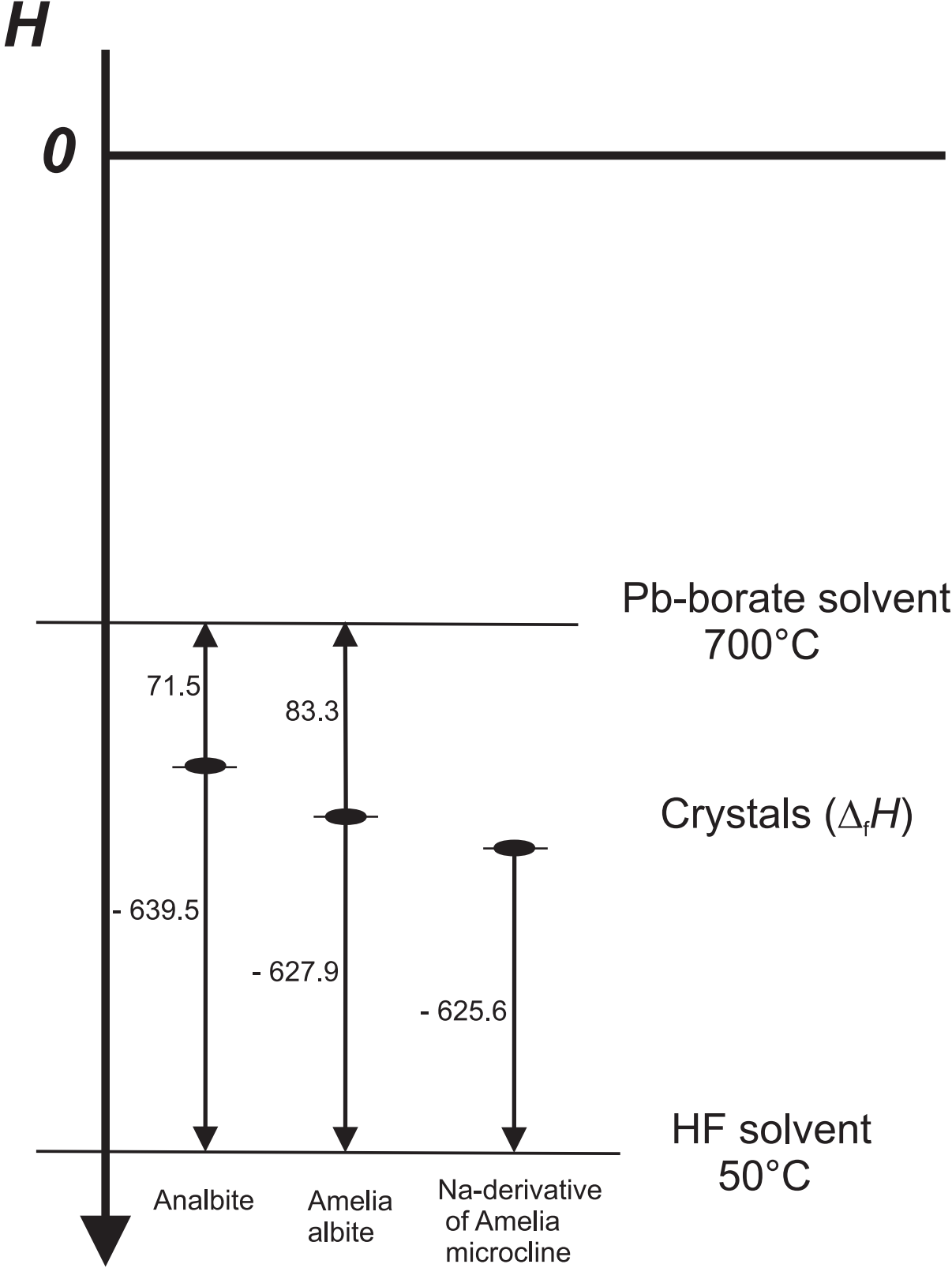


Fig. 4

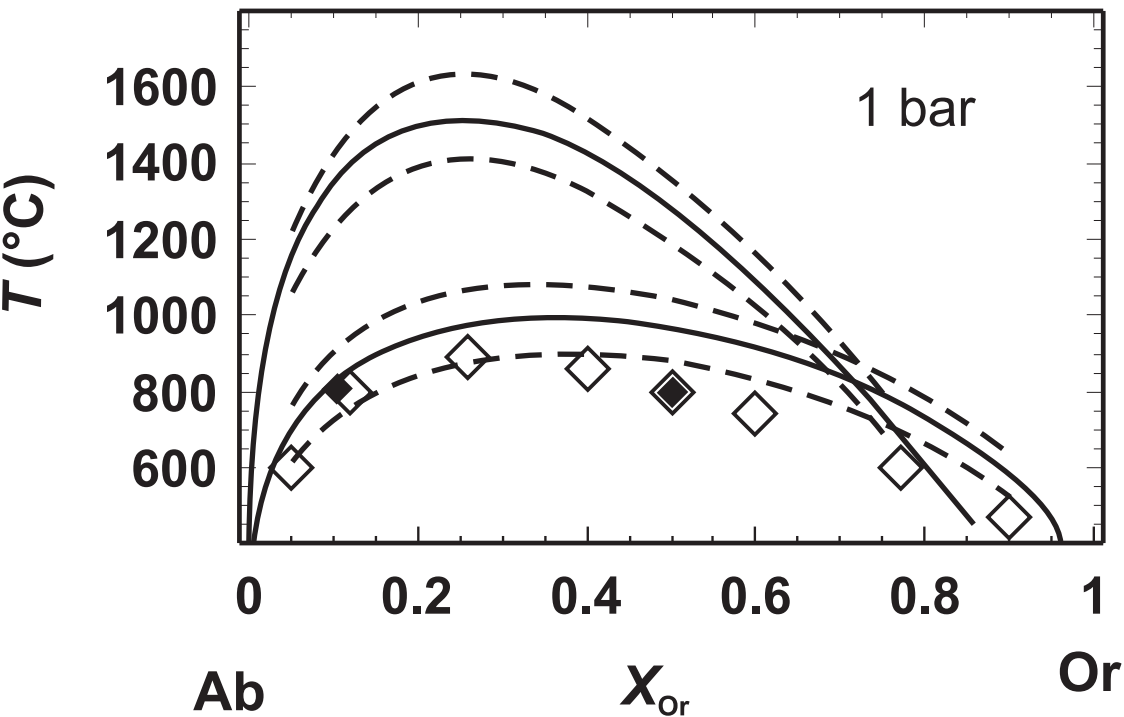


Fig. 5

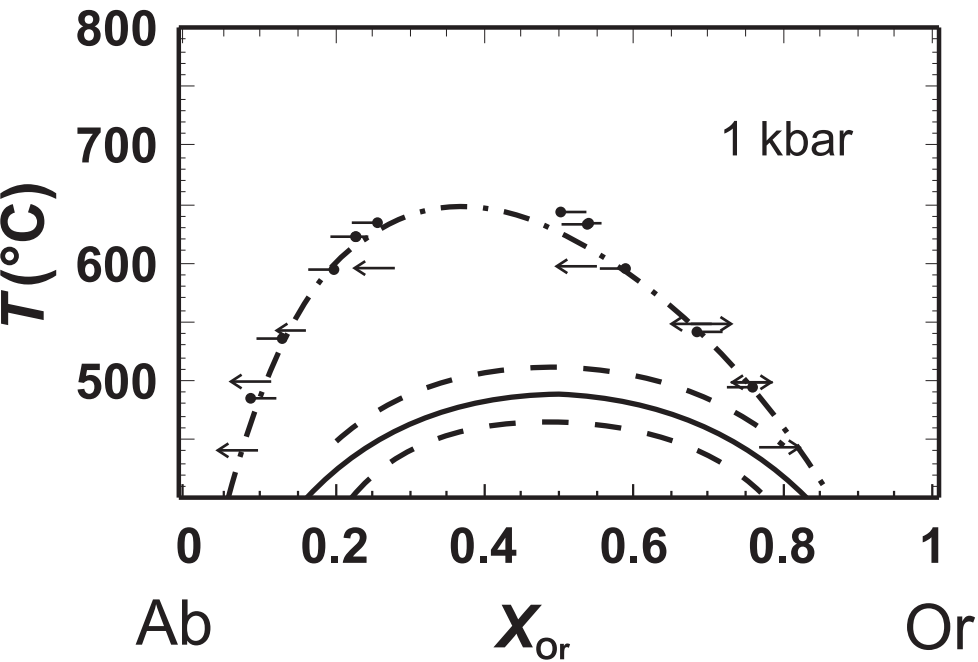


Fig. 6

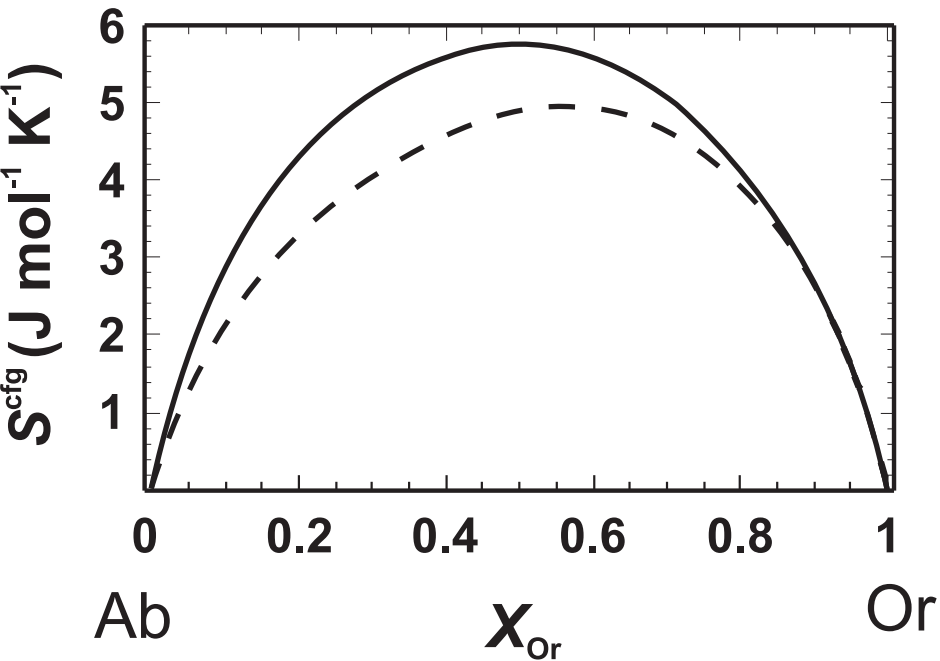


Fig. 7

Table 1 Provenance, preparation and characterisation of the two investigated ordered alkali feldspar series.

	Amelia albite series ¹⁾	Cazadero albite – Prilep microcline series ²⁾
Parent material	Amelia albite (Virginia)	Cazadero albite (California) + Prilep microcline (Macedonia)
Preparation of microcline	K-exchange of Amelia albite in molten KCl at 815°C to produce low microcline	K-exchange of Prilep microcline in molten KCl at 850°C to convert it into pure low microcline
Preparation of solid solution samples	Mechanical mixtures of Amelia albite and its K-derivative were homogenised at ~ 930°C/120h	Mechanical mixtures of Cazadero albite and K end member of Prilep microcline were homogenised at 800-1000 °C / 40-80 h
X-ray characterisation	Hovis (1988)	Kroll et al. (1986)
Transformation twinning	Not present	Present in the original Prilep microcline grains, not present in the original Cazadero albite grains

¹⁾ Prepared by Hovis (1986).

²⁾ Prepared by Kroll et al. (1986).

For more synthesis details, see their studies.

Table 2 Vibrational entropy at $T = 298.15 \text{ K}$ ($S^{298.15} - S^0$) determined in this study. The standard deviations given in parentheses refer to the last digit. The sample names are the same as in the original studies of Hovis (1988) and Kroll et al. (1986).

Samples	Or content (mol%)	$S^{298.15} - S^0$ ($\text{J mol}^{-1} \text{K}^{-1}$)
Amelia albite series		
7010	0.99	207.9 (5)
8205	16.95	209.7 (8)
8207	33.11	211.8 (4)
8047	49.26	212.8 (4)
8204	65.53	213.9 (4)
8206	82.95	214.0 (4)
71104	99.72	214.0 (4)
Cazadero albite – Prilep microcline series		
7199o	0.2	206.9 (4)
7320u	30.0	210.9 (4)
7326m	55.0	213.2 (4)
7370u	75.0	213.9 (4)
7155m	99.9	214.1 (4)

Table 3 Margules mixing parameters and equations used to calculate the activities of Ab and Or components. The sources and the parent materials are also listed.

Ordered feldspar data set 1	AbOr	OrAb	Ref.	Parent material/transformation twinning
W^H (J mol ⁻¹)	12426 ± 1757	46652 ± 1841	Hovis (1988)	Amelia albite/no
W^S (J mol ⁻¹ K ⁻¹)	8.7 ± 1.1	8.7 ± 1.1	This study	Amelia albite/no
W^V (J mol ⁻¹ bar ⁻¹)	0.619 ± 0.113	0.385 ± 0.117	Hovis (1988)	Amelia albite/no
Ordered feldspar data set 2				
W^H (J mol ⁻¹)	25899 ± 1715	35104 ± 2092	Waldbaum & Robie (1971)	Amelia microcline/yes
W^S (J mol ⁻¹ K ⁻¹)	9.1 ± 1.4	9.1 ± 1.4	This study	Cazadero albite/no + Prilep microcline/yes
W^V (J mol ⁻¹ bar ⁻¹)	0.389 ± 0.025	0.063 ± 0.038	Kroll et a. (1986)	Cazadero albite/no + Prilep microcline/yes
Disordered feldspar series				
W^H (J mol ⁻¹)	20083 ± 879	20083 ± 879	Hovis (1988)	Amelia albite/no
W^S (J mol ⁻¹ K ⁻¹)	10.3 ± 0.3	10.3 ± 0.3	Haselton et al. (1983)	Amelia albite/no
W^V (J mol ⁻¹ bar ⁻¹)	0.301 ± 0.059	0.510 ± 0.050	Hovis (1988)	Amelia albite/no

Asymmetric Margules model	$\Delta\Phi^{\text{mix}} = (1-X_K)^2 X_K W_{\text{NaK}}^{\Phi} + (1-X_K) X_K^2 W_{\text{KNa}}^{\Phi}$ $(\Phi = \text{H, S, and V})$
Mixing parameter	$W^G = W^H - T W^S + P W^V$
Activity coefficient Ab	$R T \ln \gamma_{\text{Ab}} = X_{\text{Or}}^2 [W_{\text{AbOr}}^G + 2 (W_{\text{OrAb}}^G - W_{\text{AbOr}}^G) (1-X_{\text{Or}})]$
Activity coefficient Or	$R T \ln \gamma_{\text{Or}} = (1 - X_{\text{Or}})^2 [W_{\text{OrAb}}^G + 2 (W_{\text{AbOr}}^G - W_{\text{OrAb}}^G) X_{\text{Or}}]$
Ideal activity	$a_i^{\text{id}} = X_i \quad i = \text{Ab, Or}$
Activity	$a_i = a_i^{\text{id}} \gamma_i \quad i = \text{Ab, Or}$